Journal of Materials Processing Tech. 255 (2018) 765–772

Contents lists available at ScienceDirect

Journal of Materials Processing Tech.

journal homepage: www.elsevier.com/locate/jmatprotec

Drilling-filling friction stir repairing of AZ31B magnesium alloy

Ruofei Huang, Shude Ji*, Xiangchen Meng*, Zhengwei Li

Faculty of Aerospace Engineering, Shenyang Aerospace University, No.37 Daoyi South Avenue, Daoyi Development District, Shenyang, 110136, China

ARTICLE INFO

Keywords:
Drilling-filling friction stir repairing
Magnesium alloy
Defect
Microstructure
Microhardness

ABSTRACT

Drilling and filling stages were successfully performed to produce a regular volume defect and then repair this fabricated defect. The microhardness distribution of the repaired joint was flat, and an excellent diffusion bonding occurred at the interface between the filler and the base material (BM) under the optimum combinations of a rotational velocity of 1600 rpm, dwell time of 20 s and plunge depth of 0.4 mm. A high-quality joint with the maximum tensile strength of 217 MPa was achieved. The fracture position of this joint was located at the thermo-mechanically affected zone rather than the interface between the filler and the BM of the joint with a low tensile strength.

1. Introduction

Many methods have been proposed by scholars for repairing keyhole remained in a friction stir welding (FSW) joint that is produced by retracting a rotational tool. These methods are classified into two categories as follows: a rotational pin selected as a filler material, and a pinless tool used to join an extra filler material. Du et al. (2016) performed friction plug welding (FPW) to repair the keyhole. In addition, friction bit joining (FBJ) has been proposed, in which a consumable bit was used as the filler material (Huang et al., 2009). However, a rotational filling plug (bit) had common characteristics and lacked a rotational shoulder. Under this condition, heat input was only derived from the friction between the filling plug (bit) and workpieces to be welded, thereby easily causing inadequate frictional heat and material flow, especially under low rotational velocity or small welding force. Therefore, welding defects, such as lack of bonding and cavity, easily formed in the FPW or FBJ joints. Huang et al. (2011) proposed filling friction stir welding (FFSW) in which a novel detachable tool with a rotational shoulder and a consumable filling bit was used to solve the problems induced by the absence of a rotational shoulder. The tensile strength of the sound FFSW joint reached 95% of a superior FSW joint. The keyhole in the FSW joint of stainless steel was also repaired by using the FFSW (Zhou et al., 2014). However, welding defects, such as zigzag lines and voids, easily formed at the interface between the filling bit and workpieces to be welded. Currently, the pinless tool had considerable attention because no keyhole remained at the end of the FSW joints. Zhang et al. (2014) added a filler material in the keyhole, repairing the keyhole by a pinless tool. Ji et al. (2016) proposed an active-passive filling friction stir repairing ((A-PFFSR)) technique for repairing the volume defects of FSW joints by numerous pinless tools with various shoulder diameters.

In the present study, a drilling-filling friction stir repairing (D-FFSR) technique, which was a variant of the A-PFFSR technique, was proposed to repair the volume defects adjacent to the metal structural surface. Two specially designed pinless tools with different shoulder diameters and an extra filler material were used. Microstructural evolution, material flow, hardness and tensile properties for the D-FFSR joints of AZ31B magnesium (Mg) alloy were investigated.

2. Experimental procedure

The base material (BM) used in this study was a hot rolled AZ31B Mg alloy sheet with a thickness of 3 mm, width of 180 mm and length of 200 mm. The chemical compositions and tensile properties of the BM (Table 1) are all tested by experimental analysis. The top surface of the sheet was polished with an emery paper to remove oxide layer before the D-FFSR.

Fig. 1 presents the schematic of the D-FFSR process. The volume defects with varied geometries are machined into a regular geometric shape to fill an extra material (Fig. 1a-c). The D-FFSR includes drilling, filling and retracting stages. The two pinless tools with different shoulder diameters were used during the D-FFSR process. Firstly, one pinless tool with a small shoulder diameter is used to drill a regular cylinder hole (Fig. 1b). Secondly, an extra filler with the diameter that is similar to the cylinder-shaped hole, is added to the hole (Fig.1c). The second pinless tool with a large shoulder diameter exerts frictional heat and forging force on the extra filler material for a dwell time of several seconds, as illustrated in Fig. 1d. Finally, the pinless tool retracts, and

* Corresponding authors.
E-mail addresses: superjsd@163.com (S. Ji), mengxch2013@163.com (X. Meng).

https://doi.org/10.1016/j.jmatprotec.2018.01.019
Received 17 August 2017; Received in revised form 14 January 2018; Accepted 17 January 2018
0924-0136/

Table 1
Chemical compositions and tensile properties of the AZ31B alloy.

Chemical compositions (wt, %)				Tensile properties	
Al	Zn	Mn	Mg	Tensile strength (MPa)	Elongation (%)
2.582	0.891	0.363	Bal.	240	11.2

the repairing of the volume defects is completed (Fig. 1e).

In the previous study (Ji et al., 2016), the (A-PFFSR) technique utilised numerous pinless tools with various shoulder diameters and a similar filler material, thereby repairing the keyhole defects. However, an irregular hardness distribution limited the engineering application of the repaired workpiece. Moreover, the fracture position of the repaired joint of AZ31B Mg alloy was located at the interface between the filler material and the BM, resulting from poor diffusion bonding. In this study, these two problems are attempted to be solved. According to the reported references, considerable heat input (Chang et al., 2004), extended heating time (Ji et al., 2015) and robust forging force (Aydın et al., 2012) should be used to improve diffusion bonding.

A pinless tool with a 10 mm shoulder diameter during the drilling stage was rotated anticlockwise at a rotational velocity of 1600 rpm, and a drilled hole with a depth of 1.5 mm was attained. A pinless tool with a six-spiral-groove shoulder owning a shoulder diameter of 14 mm was employed at the filling stage. The width and depth of the groove were 1 mm and 0.5 mm. A rotational velocity of 1600 rpm and a dwell time of 20 s were maintained. Four plunge depths of 0.2, 0.3, 0.4 and 0.6 mm were used. The height of the filler material was set as 2 mm to obtain a high forging force and reduce surface indentation.

Microstructural and mechanical specimens were cut from the D-FFSR joint. The microstructural specimens were prepared according to the standard procedures, which includes grinding, polishing and etching. The etching solution was composed of 10 ml CH_3COOH, 4.2 g $C_6H_2OH(NO_2)_3$, 10 ml H_2O and 70 ml C_2H_5OH. The macrostructure and microstructure were observed using an optical microscope. Tensile specimens were machined by an electrical discharge machine in accordance with GB/T 2651-2008 (equivalent to ISO 4136:2011). Schematic of the tensile specimen is depicted in Fig. 2. A tensile test at room temperature was performed at a crosshead speed of 2 mm/min. The average value of the three tensile specimens was presented for discussion. The fracture surfaces of the tensile specimens were observed using a scanning electron microscope. A conventional FSW experiment was performed under a rotational velocity of 1600 rpm, plunge depth of 0.2 mm and welding speed of 80 mm/min to discuss the tensile properties of the D-FFSR joints. A vickers microhardness tester was used to measure hardness. The testing step, testing force and dwell time were 0.5 mm, 200 g and 10 s, respectively.

3. Results and discussion

3.1. Cross-sections

In the previous experiment, the pinless tool squeezed the redundant material overflow out of the repaired zone, thus forming a regular cylinder-shaped hole at the drilling stage. Fig. 3 presents the material flow behaviour at the drilling stage and the cross section of the repaired joint after the drilling stage. The material underneath the shoulder is difficult to be squeezed out of the joint when the pinless tool does not rotate, thereby leading to the loss of the adjacent plasticised material caused by the pressing effect. Therefore, the pinless tool rotates and its rotational direction is anticlockwise based on the groove geometry on the shoulder. The materials that flow in the groove under this condition experience two forces, as demonstrated in Fig. 3a. The first force is positive pressure (p) provided by the side wall of the groove, and the second force is friction force (f) between the plasticised material and the side wall of the groove. The resultant of forces (N) transfers the materials underneath the shoulder into the shoulder edge, thus resulting in large flashes on the top surface (Fig. 3b).

The macrostructures of the repaired joints using different plunge depths are displayed in Fig. 4. Obviously, no welding defects appear in the repaired joints under the plunge depths of 0.3, 0.4 and 0.6 mm (Fig. 4b, c and d, respectively). The defects illustrated in Fig. 5 appear in the repaired joint at the plunge depth of 0.2 mm. These defects are called kissing bond (Fig. 5a), gap (Fig. 5b) and cavity (Fig. 5c). The defect-free repaired joint can be attained when the plunge depth varies from 0.3 mm to 0.6 mm. In Fig. 4, the thickness reduction of the repaired joint increases with the increase of plunge depth, which is detrimental to the quality of the joint.

In Fig. 4b, the D-FFSR joint is divided into four typical zones, namely BM, heat affected zone (HAZ), thermo-mechanically affected zone (TMAZ) and stir zone (SZ). SZ consists of filling affected zone (FAZ) and drilling affected zone (DAZ). The rotational tool stirs the materials under the shoulder when reaching the designed position at the drilling stage, thereby forming the DAZ. The pinless tool with high rotational velocity aggressively contacts and stirs the extra filler material at the filling stage, thus realizing sufficient mixing between the filler and its adjacent materials. In Fig. 6, the resultant of forces (N) on the filler material transfers the material underneath the shoulder into the centre of the FAZ when the pinless tool rotates clockwise. The accumulated materials increase at the filling stage and then partly flow downwards in accordance with the law of minimum resistance. Consequently, the material near the bottom of the FAZ flows upwards, thereby leading to the occurrence of the flashes (Fig. 4). The material flow behaviour presented in Fig. 6 is beneficial to increasing the height of the FAZ. The heights of the FAZ under the plunge depths of 0.2 and 0.3 mm are 1.3 and 1.7 mm (Figs. 4a and b). Therefore, it can be concluded that a larger plunge depth is beneficial to increasing the height of the FAZ, resulting from a large heat input, low flow stress and high material flow velocity. The spiral-groove geometry is better than a conventional concentric-circle-groove geometry in terms of increasing the material flow behaviour perpendicular to the joint surface (Zhang et al., 2011). This condition allows the use of six-spiral-groove shoulder in this study and other relative investigations (Liu et al., 2016). Moreover, the material in contact with the shoulder possesses a high flow velocity, which decreases with the increase of the distance away from the shoulder edge, thereby causing the DAZ and FAZ to present a bowl shape. Moreover, compared to the shoulder edge, the material that comes in contact with the shoulder centre undergoes a smaller linear speed and lower temperature at the filling stage. The material underneath the shoulder centre undergoes low material flow velocity and low temperature given the two above mentioned trends. The diffusion bonding under the low material flow velocity is considered as the main joining mechanism for the interface between the FAZ and the DAZ.

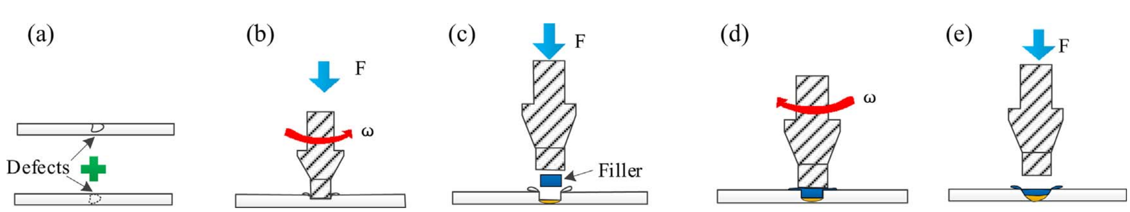

Fig. 1. Schematic of the D-FFSR process: (a) volume defects, (b) drilling stage, (c) adding fillers, (d) filling stage and (e) retracting stage.